Journal of Solution Chemistry
https://doi.org/10.1007/s10953-022-01238-z

Structural Relaxation and Thermodynamics of Viscous Aqueous Systems: A Simplified Reappraisal

Alberto Schiraldi[1]

Received: 27 September 2022 / Accepted: 28 December 2022

Abstract
The attainment of true equilibrium conditions is a dynamic process that encompasses a time span. For slow relaxing systems, non-equilibrium steady states can often look like equilibrium states. This is the case of viscoelastic systems, whose properties reflect their thermo-rheological history. After a summary of the seminal woks by Eyring, Adam & Gibbs and Angell, and mention of promising recent approaches that imply updated theoretical and experimental techniques, the paper suggests a simplified approach for aqueous systems, through a modified expression of the chemical potential of water and use of the "dynamic" phase diagram, so far proposed by Slade and Levine. For homogeneous systems (aqueous solutions), an extra term in the expression of the chemical potential accounts for the energy related to the residual strains produced during the thermo-rheological history of the system. This approach allows estimation of the effect of viscosity on the observed freezing point of polymer solutions. For heterogeneous systems (hydrogels, colloidal glasses), changes of the phase boundaries in the phase diagram explain the gel/sol hysteresis and the syneresis process as the result of water exchange between hosting meshes and trapped aqueous solution. Finally, physical hurdles that hinder inter-phase water displacements and/or the access to the headspace of the system can lead to the coexistence of aqueous phases with different a_W within the same heterogeneous system.

Keywords Aqueous systems · Viscosity · Excess entropy · Metastable states · Relaxation processes · "Dynamic" phase diagram

1 Introduction

Classical thermodynamics deals with equilibrium states, i.e., those attained once any gradient of the chemical potentials across the considered system vanishes. The attainment of true equilibrium conditions is a dynamic process that encompasses a time span during which long-range strains and dishomogeneities relax. That is why for slow relaxing systems non-equilibrium steady states can often look like equilibrium states. This is the case of soft materials, like many food products, animal and vegetal tissues, gels, etc.:

✉ Alberto Schiraldi
alberto.schiraldi@unimi.it

[1] DeFENS, University of Milan, Milan, Italy

Published online: 23 January 2023

they are viscoelastic systems, showing a behavior that substantially changes with the temperature. The preparation procedure (e.g., stirring, kneading, mixing, etc.) produces structural strains coupled with short- and long-range heterogeneous regions, which can remain for long periods. Quenching below a critical threshold (glass transition) makes any molecular displacement "frozen" and favors the persistence of these strains. The material becomes fragile and brittle. Examples are frozen food and frozen tissues. Heating above a threshold (glass–rubber, rubber–liquid, gel-sol transition) makes these strains relax partially. The system first becomes plastic (i.e., keeps some deformation after the removal of a shearing stress) and, at higher temperatures, it becomes a viscous fluid that flows in the direction of the applied stress. Plasticity and viscosity thence reflect strains within the structure. Relaxation of these strains implies release of some energy (either as heat or as mechanical work). This means that retained strains are tantamount to an additional potential energy that tends to vanish when they relax.

It is known that relaxations at the molecular scale encompass time windows (from 10^{-15} to 10^{-3} s) that are much narrower than the macroscopic scale ($10^{(n \geq -2)}$ s). The latter are relevant to properties of the whole system, like heat capacity, entropy, density, water activity, elastic modulus, viscosity, etc. Any correlation between processes at the molecular scale, with very short relaxation times, and those dealing with isotropic properties at the macroscopic scale, with much longer relaxation times, usually requires statistical or molecular dynamics approaches.

As for aqueous systems, the traditional approach puts $a_W = X_W\ \gamma_{a,W}$ (where a_W, X_W and $\gamma_{a,W}$ stand for: water thermodynamic activity, molar fraction and activity coefficient, respectively). Polynomial (often dubbed "virial") expressions allow the fit of the $\gamma_{a,W}$ values calculated from a_W experimental data. Each term of the virial expression is a power of X_W and reflects a specific solute–solute or solute–solvent interaction, according to the selected model to describe the system [1]. This is tantamount to relating thermodynamic properties of the whole system to structure peculiarities and molecular interactions, which normally imply different scales for the related relaxation times. The relevant connection between macro- and micro-scale is the "model" used with the assumption of a Boltzmann distribution of the accessible states and the ergodicity of the system.

A measure of the structural strains experienced by an aqueous solution that slowly flows in a tube is the relative viscosity, $\eta_r = \eta/\eta^*$ (where "*" stands for pure solvent), that can be determined with an Ubbelohde viscometer. The η/η^* ratio reflects the change of the ability of the system to flow because of the presence of the solute. In this case too, polynomial and empirical relationships are proposed for the η_r vs X_W trends [2], with an interpretation of the X_W powers rather similar to that for $\gamma_{a,W}$. Thence, one could be inclined to draw an a_W vs η_r expression from the a_W vs X_W and η_r vs X_W empirical relationships.

The experimental evidence shows that such a correlation may be difficult to justify for aqueous solutions (Fig. 1), which show, at a given temperature, rather different a_W vs X_W and η_r vs X_W trends. a_W practically does not depend on the kind of solute, as expected for a thermodynamic, namely "static", property, while η_r shows solute-related trends, that mainly depend on the relevant steric hindrance, as expected for a "dynamic" property.

However, thermodynamic equilibrium and any steady metastable state is not a "static" condition at the molecular level, being the result of local fluctuations that imply displacements and back relaxations of molecules governed by the local hindrance of the medium (see below). This means that the distinction between "static" and "dynamic" depends on the time scale considered.

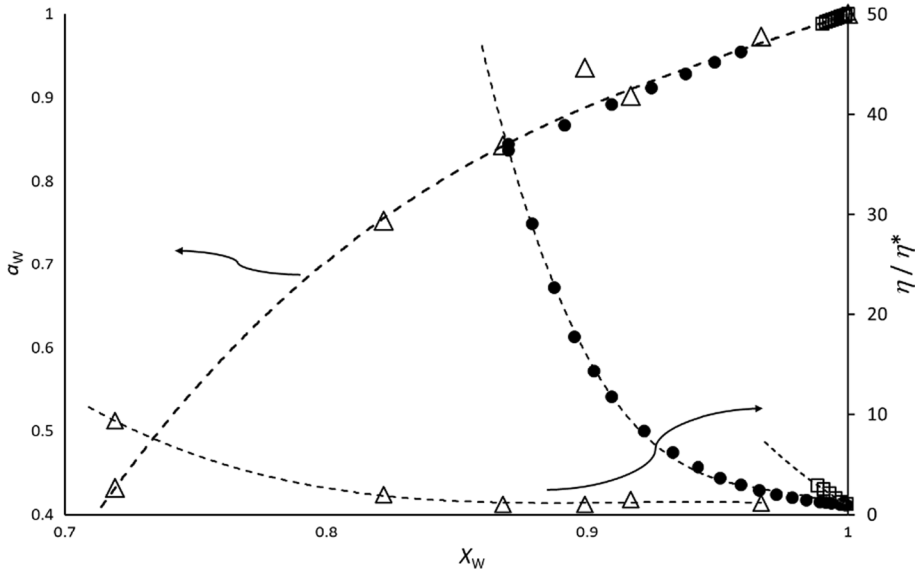

Fig. 1 At 25 °C, water activity, a_W, shows practically the same trend for: saturated electrolytes (K_2CO_3, NaCl, KCl, $BaCl_2$, KNO_3, K_2SO_4) [3, 4], triangles, D-glucose [3], full dots, and PEG 400 [5], squares, while substantial differences appear for the respective relative viscosities (right hand axis). Water molar fraction X_W (assuming complete dissociation of salts) replaces the concentration units of the original data

For poorly viscous aqueous solutions, an applied shear tress, τ, mainly produces flow, since any structural long-range strain, γ, relaxes quickly. For soft materials, an applied stress mainly produces strains with long relaxation times, typical of the viscoelastic behavior. Increasing T favors the former condition and crossing the rubber–liquid threshold makes the soft material behave as a viscous fluid.

Long-range strains within the system depend on its thermo-rheological history and affect its internal energy for periods that are much longer than the relaxation times of processes at the molecular scale. However, the relaxation mechanism of long-range strains implies a concerted cooperation of short-range relaxations within mesoscopic regions of the system [6]. This justifies the search of a correlation between local relaxation processes, in the so-called zero shear conditions, and thermodynamic excess properties, like excess configuration entropy or excess Gibbs free energy. The relevant models therefore are “static” or “quasi-static”.

2 Scope of the Work

The first part of the present work briefly summarizes the “state of the art” reporting the main relationships between viscosity and excess thermodynamic properties of homogeneous systems, since the seminal works by Eyring, Di Marzio, Adam and Gibbs, and Angell to the more recent approaches that highlight the need to account for different time scales to describe the relaxation processes. The second part of the paper aims to suggest a simplified phenomenological approach by use of a modified expression of the chemical potential of water and the expected changes of the so-called supplemented or dynamic phase diagram

for aqueous homogeneous (solutions) and heterogeneous (hydrogels and dispersed multiphase) systems.

3 The State of the Art

Most of the papers that suggest a correlation between zero-shear η and thermodynamic properties are based on the seminal works by Di Marzio and Adam and Gibbs (AG) [7–9] who proposed a model for glass-forming liquids that relates structural relaxations at the molecular level with long wave relaxation processes that involve the whole system at the macroscopic scale. The most mentioned expression of the AG model is as follows:

$$\tau_{\mathrm{R}} = \tau_{\mathrm{R}}(\infty)\exp\left(\frac{C}{TS_{\mathrm{c}}}\right), \tag{1}$$

where $\tau_{\mathrm{R}}(\infty)$ is the relaxation time at $T=\infty$, and S_{c} is the molar configurational entropy of the system with respect to a stable solid state. Using the Maxwell relationships [10], $G(t) = G_{\infty}\exp(-\frac{t}{\tau_R})$ and $\eta=\tau_{\mathrm{R}}\, G(\infty)$, where G is the shear modulus, Eq. 1 becomes [11],

$$\eta = \eta(\infty)\exp\left(\frac{C}{TS_{\mathrm{c}}}\right) \tag{2}$$

which apparently correlates η with S_{c} that is a thermodynamic property of the system. It is important to remind that, in Eq. 2, $\eta=(\tau/\dot{\gamma})$ is the zero-shear viscosity, namely the extrapolated value of $(\tau/\dot{\gamma})$ for either quantity tending to zero.

Both Eqs. 1 and 2 are expressions for relaxation processes at supra molecular level ("cooperative regions" [7, 8]) that enlarge to macroscopic size on decreasing T [8, 9].

It must be noticed that the true concern of Adam and Gibbs was "the temperature dependence of relaxation phenomena in glass-forming liquids… essentially in terms of the temperature dependence of the size of the cooperatively rearranging region", which "is shown to be determined by the configuration restrictions associated with amorphous packing … described by the configurational entropy of the melt" [8].

The same authors [8] showed that their model leads to an expression for the ratio of relaxation times, a_T, at the temperatures T and T_{g} (glass transition temperature), which agrees with the WLF empirical equation [12],

$$-\log\left(a_T\right) = \frac{C_1\left(T-T_{\mathrm{g}}\right)}{C_2+\left(T-T_{\mathrm{g}}\right)} \tag{3}$$

provided that no "universality" is attributed to the values of C_1 and C_2. Equation 3 directly reflects the Boltzmann time–temperature superposition principle, which allows prediction of properties detected at low shear rate, $\dot{\gamma}$, at the temperature T_2 from those detected at larger shear rate at the temperature T_1. This may be the reason why, despite its "quasi-static" [8] character, Eq. 3 can apply to relaxation processes corresponding to a prevailing loss component of the macroscopic shear modulus, G'', directly related to the viscosity of viscoelastic systems, as $\eta=G''/\omega$ (ω standing for the frequency of the applied oscillating strain or the shear rate). One therefore may replace a_T in Eq. 3 with the ratio $[\eta(T)/\eta(T_{\mathrm{g}})]$, provided that the viscosity values are independent on $\dot{\gamma}$ and correspond to a Newtonian-like behavior [7–9].

With this constraint, Eq. 3 allows description of the η vs T trends of a number of liquid systems above their glass transition thresholds. Many experimental trends observed for aqueous solutions of salts, sugars and polymers [13] seem better described with the VTF empirical equation [14], although straightforward algebraic relationships reconcile WLF and VTF equations if C_1 and C_2 have no "universal" values [15] (see Appendix).

Angell [16–18] proposed the picture of "strong" and "fragile" liquids as an enhancement of the Adam and Gibbs model, as far it describes the empirical evidence of the non-Arrhenius dependence of the viscosity and the electrical conductivity of many liquids. The representation of experimental data uses the scaled temperature (T_g/T) assuming that the condition attained at T_g implies a quasi-iso-viscous, or iso-relaxation state of liquids.

A more "dynamic" model for the viscosity of liquids comes from the Eyring's proposal [19, 20] of an "activated" mechanism for flowing systems that corresponds to the expression of the absolute rate of reaction by the same author [19] and its extension to viscosity and diffusion [20]. Eyring's model reflects those proposed in the same decade by Shottky [21] and Frenkel [22] to describe the diffusion of point defects in ionic solids. The jump mechanism underlying the mobility at the molecular scale in liquids would not imply any neat displacement of the jumping particle, as forward and backward direction of successive jumps have equal probability. The crucial role of an ad hoc factor, $0 < k \leq 1$, is to favor the jumps in the direction of the driving force that sustains the displacement of the whole system or its flow in a given direction. The k factor makes an otherwise quasi-static picture a kinetic model of transfer.

This approach found general support in works where viscosity data collected at various temperatures allowed estimation of an activation Gibbs energy, split in enthalpy and entropy contributions [23].

$$\eta = P \exp\left(-\frac{\Delta S^*}{R}\right) \exp\left(\frac{E_{att}}{RT}\right) \tag{4}$$

where P is a pre-exponential factor. A non-negligible "activation entropy", ΔS^*, and its dependence on T are supposed to be responsible for the deviation from the Arrhenius behavior of many glass-forming systems, which show a smaller than expected decrease in η on increasing T: which looks like an embryonal picture of the "fragility" defined by Angell.

More intriguing and appealing seems the approach that relates thermodynamic equilibrium to the time scale considered [6, 24–28]. Assuming the ergodicity of the system, this approach allows a connection between long wave relaxation processes that deal with the viscoelastic behavior and thermodynamic properties of many materials, which imply two time scales, one related to the linear dependence on time of the mean squared displacement, the other related to the Gaussian distribution of the particle displacements. Further developments of this approach eventually lead to the description of the non-equilibrium condition met in most soft materials that show a viscoelastic behavior and a memory of their thermo-rheological history, because of structural arrangements, produced by decreasing the temperature or applying mechanical stresses, with possible loss of ergodicity (see [29] for a wide survey of this subject). It is worth noticing that the relevant formal description requires in many cases advanced mathematical tools, including fractional differentiations [29] and physical theories proposed for complex systems [30–32].

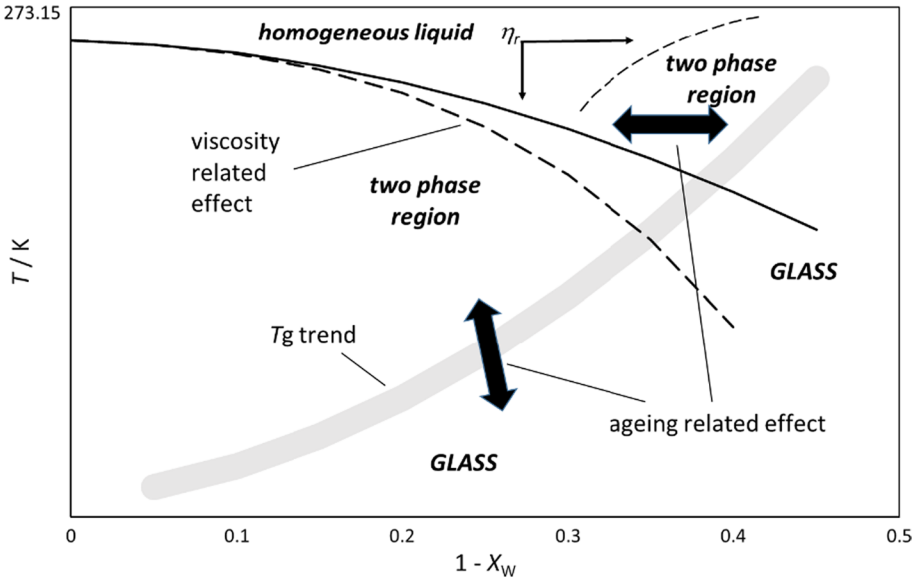

Fig. 2 Phase diagram of an aqueous system. X_W is the water molar fraction. The cross-point between the trends of the glass transition temperature, T_g, and the freezing curve corresponds to the maximally freeze-concentrated liquid phase. The relative viscosity, η_r, of the liquid phase increases either by isothermal drying or by cooling. Viscosity and aging (black arrows) produce substantial effects on the phase boundaries

4 An Alternative Approach

The "dynamic" phase diagram, proposed 30 years ago by Slade and Levine as a fundament of the Food Polymer Science [33] and more recently reviewed as "supplemented" phase diagram [34], reports the trend of the glass transition temperature, T_g, vs the composition, C_W (water mass fraction), at constant pressure. The cross-point between freezing and T_g trends, (C_g', T_g') corresponds to the lowest temperature for a homogeneous liquid phase. Formally defined for an aqueous binary, such a diagram can represent the phase map of a pseudo-binary, as far as $(1-C_w)$ can gather the mass fractions of all the non-water components of the system. This phase diagram reports the boundaries between phases, but does not provide any connection with the relevant viscosities, which nonetheless play a crucial role on their trends. This is the case of aqueous polymers and aqueous gel formers, for which a rest condition, that (depending on temperature, thermo-rheological history and age of the system) can last for a long time, but does not necessarily correspond to a true thermodynamic equilibrium. Figure 2 reports a sketched view of the effects of viscosity and aging on the trends of the phase boundaries. For a given molar fraction of water, X_W, cooling produces an increase in the relative viscosity of the homogeneous liquid phase, which means a decreased probability of forming crystal nuclei and ice growth, and on the solubility trend (dotted line in Fig. 2). Aging implies shift of the T_g and solubility trends because of water exchanges between coexisting phases (see below). Such shifts modify the coordinates of the maximally concentrated liquid phase.

Steady metastable states are indeed possible which slowly relax towards an eventual state that can still be metastable [35]. When so, some extra energy remains within the system as an

excess Gibbs energy associated with residual strains or structural rearrangements (shear thinning and shear thickening) generated during a previously experienced stress. This is why the Gibbs free energy and any measured property of the system reflect an instantaneous state and therefore depend on the "waiting time" [35], namely the time gap between preparation and investigation.

4.1 Homogeneous Aqueous Phases

One can try to account for the deviation from the true equilibrium by modifying the classical expression for the chemical potentials. As for water,

$$\mu_{\mathrm{W}} = \mu_{\mathrm{W}}^{*} + RT \ln a_{\mathrm{W}} + \mu_{\mathrm{visc}} \tag{5}$$

where μ_{visc} stands for the residual strain energy entrapped within the system.

In a steady condition that can mimic a true thermodynamic equilibrium, one can apply the Adam–Gibbs relationship and rewrite the term μ_{visc}, choosing the pure solvent as reference state, namely

$$\ln\left(\frac{\tau_{\mathrm{R}}}{\tau_{\mathrm{R}}^{*}}\right) = \frac{\left(\overline{C/S}_{\mathrm{c,W}} - C^{*}/S_{\mathrm{c,W}}^{*}\right)}{T} \propto \ln\left(\frac{\eta}{\eta^{*}}\right) \tag{6}$$

where "*" stands for pure solvent. Finally, one can rewrite Eq. 5

$$\mu_{\mathrm{W}} = \mu_{\mathrm{W}}^{*} + RT \ln a_{\mathrm{W}} + RT \ln\left(\frac{\eta}{\eta^{*}}\right)^{\alpha(T,p,N,t)} \tag{7}$$

The exponent $\alpha \geq 0$ would depend on temperature, T, pressure, p, kind (polymers, small mass compounds, polar molecular moieties, etc.) and concentration, N, of the solute, and on the "waiting time", t.

For dilute aqueous solutions of salts or simple sugars at room temperature, no significant strains remain when the applied stress is withdrawn, namely $\alpha = 0$. However, for temperatures close to the freezing point, η^{*} would represent the viscosity of undercooled liquid water and $\eta \gg \eta^{*}$. In such condition, one may not neglect the term μ_{visc} that, using Eq. 7, becomes

$$\mu_{\mathrm{visc}}(T) = RT\alpha \ln\left(\frac{\eta}{\eta^{*}}\right) = RT\beta(T) \approx \alpha R\left(\frac{C}{S_{\mathrm{c}}} - \frac{C^{*}}{S_{\mathrm{c}}^{*}}\right) > 0 \tag{8}$$

One may accordingly write

$$\mu_{\mathrm{W}} = \mu_{\mathrm{W}}^{*} + RT\left[\ln a_{\mathrm{W}} + \beta(T)\right] \tag{9}$$

This expression leads to predict that the freezing point expected for $\beta(T) = 0$ (namely, neglecting the effects of viscosity), T_{f}, is above the actually observed one, T_{f}', for any given composition of the liquid phase,

$$\left(T_{\mathrm{f}} - T_{\mathrm{f}}'\right) = \beta(T)\left(R\frac{\left(T_{\mathrm{f}}^{*}\right)^{2}}{\Delta_{\mathrm{fus}}H^{*}} + \cdots\right) \geq 0 \tag{10}$$

For a given composition of the liquid, X_W, cooling produces an increase in the viscosity. Since, for a given temperature, η increases with increasing $(1-X_W)$, the $\left(T_f - T_f'\right)$ difference increases on cooling. The function $\beta(T)$ must therefore be null for $T=T_f$* (* stands for pure water), and increase on decreasing X_W.

A dramatic example of the effect of viscosity on the freezing point is the case of aqueous arabino-xylans, well known for their exceptionally large viscosity even at very low concentration. For high (410 kDa) and low (52 kDa) number average molecular weight arabino-xylans (HMW and LMW) T_g‘ = − 17 °C and − 35 °C, respectively, while in either case the water mass fraction is C_g‘ ≈ 0.75 [36] (which nonetheless corresponds to different polymer molar fractions [36]).

These data allow a rough estimation of the $\beta(T)$ values at the respective T_g'. Applying Eq. 10, one can easily realize that the depression of the freezing point mainly depends on the viscosity, as $X_W \approx 1$ for either polymer solution, and that for $T=T_g'$

$$T_g' = 273.15 - \beta\left(T_g'\right)R\frac{\left(T_f^*\right)^2}{\Delta_{fus}H^*} \tag{11}$$

which yields $\beta(T_g')_{HMW} \approx 0.17 \approx 0.5\ \beta(T_g')_{LMW}$. If one assumes that the (C_W', T_g') state implies the same viscosity for both polymers, as in either case this is the point where the formation of ice nuclei ceases, then

$$\ln\left(\frac{\eta_{HMW}}{\eta_{LMW}}\right)_{T=T_g'} = \left(\frac{\beta_{(Tg')HMW}}{\alpha_{HMW}} - \frac{\beta_{(Tg')LMW}}{\alpha_{LMW}}\right) = 0 \tag{12}$$

which means that $(\alpha_{HMW}/\alpha_{LMW})_{Tg'} \approx 0.5$.

Equation 8 allows an estimation of the difference between the values of μ_{visc} at the two T_g', $\Delta\mu_{visc} \approx 13\ J \cdot mol^{-1}$, namely an almost negligible value, in line with the assumption that the (C_g', T_g') state actually is an iso-viscous condition.

For concentrated aqueous solutions, especially of polymers, η would change with the system aging and depend on the previous thermo-rheological history. Applying the Gibbs–Duhem relationship,

$$\frac{\mu_{visc}}{RT} = \frac{\mu_{visc}\left(T=T_g'\right)}{RT_g'} + \frac{H_{visc}}{RT_g'}\left(\frac{T_g' - T}{T}\right) = \ln\left(\frac{\eta}{\eta^*}\right)^{\alpha} \geq 0 \tag{13}$$

or

$$\frac{\mu_{visc}\left(T=T_g'\right) - H_{visc}}{RT_g'} + \frac{H_{visc}}{RT} = -\frac{S_{visc}\left(T=T_g'\right)}{R} + \frac{H_{visc}}{RT} = \ln\left(\frac{\eta}{\eta^*}\right)^{\alpha} \tag{14}$$

This leads to:

$$\ln\left(\frac{\eta}{\eta^*}\right)^{\alpha} = \left(-\frac{S_{visc}\left(T=T_g'\right)}{\alpha R}\right) + \frac{H_{visc}}{\alpha RT} \tag{15}$$

and

$$\eta(T) = A \exp\left(\frac{H_{\text{visc}}}{\alpha R T}\right) = A \exp\left(\frac{B}{T}\right) \tag{16}$$

where $A = \eta_{\infty}^{*} \exp\left(-\frac{S_{\text{visc}}\left(T=T_g'\right)}{\alpha R}\right)$ and $B = \left(\frac{C^*}{S_c^*} + \frac{H_{\text{visc}}}{\alpha R}\right)$, having applied the Adam & Gibbs expression (Eq. 3) for the viscosity of pure water. Equation 16 corresponds to the expectation for "strong" liquids [16] and to the Eyring's model (Eq. 4) when neither A nor B depends on T.

4.2 Heterogeneous Aqueous Systems

Aqueous systems, like gels, pastes and doughs, etc., in spite of the macroscopic homogeneous appearance, actually are heterogeneous. Many of these systems almost do not flow at all when experience a mild shear stress, showing a viscoelastic character, mainly related to the non-water components that host a poorly viscous aqueous solution. In hydrogels, water occupies the voids left by the entanglements of polymer chains, or the meshes of pseudo-lattice arrays of hydrated solute molecules, from where it can squeeze out once a sufficient stress reduces the volume of such watery pouches. On applying stresses or strains, what actually flows within a gel is a solution that can diffuse through the meshes and pores of the framework, which is practically immobile with respect to water and small mass solutes.

Some examples can be of interest. Overmixing a flour dough stretches its gluten meshes expelling part of their water content [37] that can evaporate more easily on baking: the final product is drier, harder and crispier. If the overmixed dough remains at rest for a couple of hours, it relaxes back and allows the re-uptake of water into its meshes [38]: the entrapped water meets some hurdles to evaporate and the final baked product is heavier, softer and gummier [39]. Many aqueous gels undergo syneresis, a process during which the resting gel, under the force of its own weight, releases a much less viscous aqueous solution. The dehydration reflects the percolation through pores and channels of the hosting structure and leads to a modest shrinkage of the system that can eventually collapse missing the mechanical support of the entrapped aqueous phase. This isothermal process is spontaneous and corresponds to an increase in entropy and a decrease in the viscosity of the aqueous phase, as confirmed in micro-rheology investigations based on Dynamic Light Scattering experiments where multiple scattering are analyzed through Diffusing Wave Spectroscopy [40, 41].

The gel–sol transition of the so-called physical gels too implies changes of entropy and viscosity. One can describe the gel formation and its evolution by considering the "dynamic" nature of the phase diagram of the system (Fig. 3).

The gel formation occurs within the biphasic region of the diagram between the glass transition and the solubility trends. The process starts at the "gel point", $T_{\text{gel on cooling}}$, on cooling a homogeneous liquid. This threshold actually depends on the cooling rate and reflects the viscosity increase in the sol phase, which hinders the displacements of the gel forming compound(s) favoring the formation of an early soft meshwork. A further cooling below $T_{\text{gel, cooling}}$ and during the rest at T_{room}, the aqueous phase becomes richer in water at the expenses of the hydrated amorphous component, which becomes drier and stiffer. This implies that the viscosity of the aqueous phase would decrease (see Fig. 2), while the amorphous component rearranges its structure to build a stiffer meshwork, at constant overall composition of the system (full circle in Fig. 3). This explains the high diffusivity of the aqueous phase that leaves the system during the syneresis. In the phase diagram, this

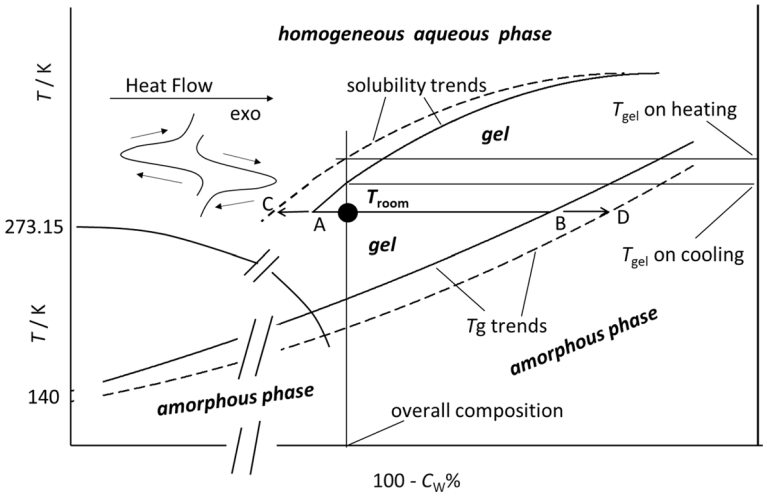

Fig. 3 Dynamic phase diagram of a hydrogel forming system. The formation of the hydrogel occurs within the two-phase region between the T_g trend and the solubility curve. At room temperature, the limits A and B of the tie line define the composition of the two phases of the gel (full dot). However, these limits change toward C and D during the rest at this temperature. On heating the gel, the transition occurs at higher temperature. The insert shows the expected DSC record of a cooling/heating cycle

transformation corresponds to the shift of the limits *A* and *B* of the early tie line toward the new limits C and D (Fig. 3). This is tantamount to modify both the T_g and the solubility trends (dotted lines in Fig. 3). In other words, the phase diagram of the system before the formation of the gel differs from the phase diagram after the formation of the gel (from continuous to dotted lines, Fig. 3). This is why, on heating, the transition to the "sol" state occurs at higher temperature, $T_{gel,\ heating}$. If the overall water content remains unchanged and the gel is really "reversible", heating above $T_{gel,\ heating}$ implies the moisture re-uptake by the amorphous component (hydration shell), which is again solubilized.

The cooling/heating DSC cycle would show an exothermic and an endothermic signal with practically equal thermal effect, $|\Delta_{gel}H|$, at $T_{gel,\ cooling}$ and $T_{gel,\ heating}$,

A qualitative (as the effect of the cooling rate is neglected) treatment of the available data ($\Delta_{gel}H$, $T_{gel,\ cooling}$ and $T_{gel,\ heating}$) allows a rough estimation of the excess configurational entropy. The experimental finding suggests that the exo- and endothermic effects have practically the same absolute value, $\lfloor\Delta_{gel}H\rfloor$.

Putting $T_{gel,\ cooling} = T_1$ and $T_{gel,\ heating} = T_2$,

$$\text{Transition entropy}: \quad \Delta_{sol/gel}S = \frac{\lfloor\Delta_{gel}H\rfloor}{T_{gel}} = \begin{cases} \Delta_{sol/gel}S_{cooling} = \dfrac{\lfloor\Delta_{gel}H\rfloor}{T_1} \\ \Delta_{sol/gel}S_{heating} = \dfrac{\lfloor\Delta_{gel}H\rfloor}{T_2} \end{cases} \tag{17}$$

$$\text{Excess configuration entropy:} \quad S^{exc}_{conf} = \frac{\lfloor\Delta_{gel}H\rfloor}{T_1} - \frac{\lfloor\Delta_{gel}H\rfloor}{T_2} = \left|\Delta_{gel}H\right|\left(\frac{1}{T_1} - \frac{1}{T_2}\right) \tag{18}$$

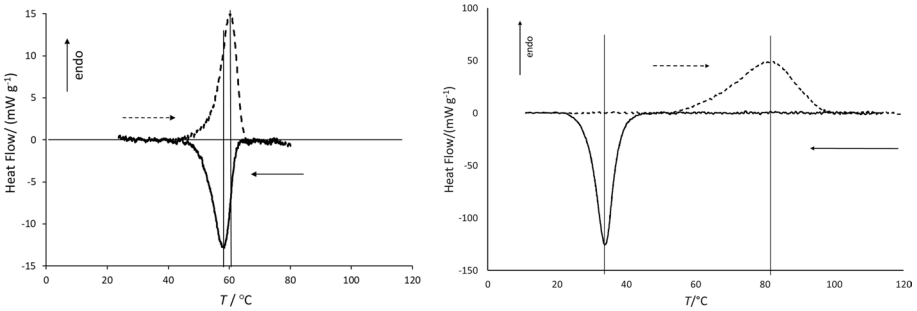

Fig. 4 DSC cooling/heating scans of Xanthan/Konjac Gluco-Mannan (left) adapted from [42] and Aga-Agar gels (right) [43]. Vertical lines evidence the width of the respective hysteresis

Equation 18 suggests that the excess configuration entropy would be much smaller than the transition entropy and mainly depend on the difference $(T_2 - T_1)$. The width of the gel–sol hysteresis would therefore reflect the excess configuration entropy, related to the local strains and stresses within the hosting amorphous meshes.

To give the order of magnitude of this entropy, one can use the data collected from two different hydrogels, Xanthan/Konjac Gluco-Mannan (X—KGM, 0.34% dry matter) [42] and agar–agar gels (0.8% dry matter) [43], respectively (Fig. 4).

As for $\Delta_{sol/gel}S$, 36 and 78 $mJ \cdot g^{-1} \cdot K^{-1}$ (dry polymer) can be roughly estimated for X-KGM and Agar gels, respectively. The observed heating/cooling hysteresis in the relevant DSC trace (Fig. 4) is about 2 K and 50 K wide (peak-to-peak) for the X-KGM and Agar gel, respectively. This leads to the estimation of S^{exc}_{conf} (Eq. 20), 0.2 and 12.6 mJ $g^{-1} \cdot K^{-1}$, namely about 1% and 16% of the transition entropy, for the X-KGM and Agar gel, respectively.

Now, some simulations of the structural conformations of the X-KGM system [42] reveal that the intermolecular assembly in the sol phase is almost equal to that in the gel phase, when the Xanthan/Konjac mass ratio is close to 1: this is in line with the small width of the gel/sol hysteresis and the small estimated excess configuration entropy. The wide hysteresis observed in the case of Agar gel would instead reflect a large degeneration of accessible conformations [44, 45] in the gel structure.

Similar approaches for the phase diagram of starch [46] are in line with the expected supramolecular interactions and changes of molecular conformations [47, 48].

Multi-phasic systems, which can host aqueous droplets, microbial cells, tissues, suspended bodies, etc., behave as supercooled liquids and undergo similar relaxation processes that depend on either the water content or the temperature [49]. Actually, some of these systems show a glass-like rheological behavior, especially for what concerns the temperature range close to the glass transition threshold. This is why they are "colloidal glasses" [50]. Experimental and theoretical simulations [51, 52] indicate the need of various time scales to define all the relaxation processes [52] and the conditions that allow the system to flow.

The different phases may appear as dispersed micro- or nano-domains, each containing some thousands of water molecules. Water can migrate through the phase boundaries, if these are permeable, and equilibrate its chemical potential throughout the system allowing the detection of a reliable value of water activity, a_W. However, it can indeed happen that, because of the hindered displacements of water molecules, some water remains concealed

within a given environment and does not contribute to the overall relative humidity, $RH \sim (a_W \times 100)$, of the system. Leathers and animal/vegetal tissues, some industrial ice creams poured into fat coated wafers, wrapped candies,[1] etc., can host regions with different a_W [53]. Of special interest are the $W_1/O/W_2$ nano-emulsions (where composition and a_W may be different in the two aqueous phases) and the cytoplasm of living cells that is much more similar to a gel than to a concentrated aqueous solution. Here, the molecular crowding [54] and the phase separation (governed by the thermodynamic incompatibility of different polymers [55]) strongly limit the mobility of water molecules. Not to say of the water exchanges between intra- and extra-cellular environments across the cell wall, governed by osmotic and oncotic effects, and affected by the mechanical tension of the membrane and by the energy consuming ionic pumps. Any value of a_W determined with isopiestic, or Knudsen [3] investigations would reflect only the a_W of the phase that has a direct access to the head space of the system, ignoring phases that cannot exchange water with the former and can have either lower or higher a_W.

For such systems, one therefore has to account for the physical constraints, like poorly porous membranes, lipid layers, dispersion in hydrophobic mediums or other hurdles that can make the displacement of water difficult, or even impossible. The experimenter needs different methods to get some information about the state of water in each single phase. Reasonable choices can be MR Image and/or MR Relaxometry which allow ranking of water mobility, u_W, of the different "water families" coexisting in heterogeneous systems [56–61]. A NMR investigation would reveal that some kind of segregated water can indeed be mobile with an activity not too far from unity, as survival and growth of microbes within a polymeric medium of apparently low relative humidity (32%) indicate [62, 63].

In such cases, rheological and thermodynamic properties seem irreconcilable with each other, as the former mainly depend on the stiffest phase, which often shows a viscoelastic and, possibly, not isotropic behavior, while the latter mainly concerns the dispersed homogeneous liquid phases.

In view of the above arguments, one may try to account for such hurdles by including a new extra term in μ_{visc}. Taking into account Eq. 7, for each homogeneous phase within the heterogeneous system, one can write

$$\mu_{visc} = RT \ln \left(\frac{\eta}{\eta^*} \right)^{\alpha} - RT \ln(H) \tag{19}$$

The $RT\ln(H)$ term deals with the hurdles ($H > 1$) that hinder the access either to the headspace or to the water exchanges between next neighboring phases, but may also account for preferential diffusion paths ($0 < H < 1$), like pores and channels at mesoscopic level, which favor percolation processes.

The first term of Eq. 19 is proportional to the logarithm of the relative viscosity of the aqueous phase which is a function of the solute concentration, $\ln(\eta_r) = F(c)$, like in the Jones and Dole equation [2]. A more detailed expression has to account for all the interphase boundaries within the heterogeneous system. For the ith aqueous phase of a n-phase heterogeneous system,

[1] "*A difference in water activity, either between candy and air or between two domains within the candy, is the driving force for moisture migration in confections. When the difference in water activity is large, moisture migration is rapid, although the rate of moisture migration depends on the nature of resistances to water diffusion. Barrier packaging films protect the candy from air whereas edible films inhibit moisture migration between different moisture domains within a confection.*" [53].

$$\mu_{\mathrm{W},i} = \mu_W^* + RT \ln \left(a_{\mathrm{W},i} F_i\right) - RT \ln \sum_j^n h_{ij} \tag{20}$$

where F_i stands for $\left[F\left(c_i\right)\right]^{\alpha_i}$, and the parameters h_{ij} reflect the inter-phase exchanges, with $h_\mathrm{ij} \geq 0$ ("=" for not next neighboring phases) and $h_{ii} = 1$. The h_{ij} term actually is a vector directed from the phase i toward the phase j: thus $h_{ij} \neq h_{ji}$ if the water displacement encounters different hurdles in the two directions. For a heterogeneous system hosting n aqueous phases, a general steady condition (namely, no neat inter-phase water displacements) therefore is as follows:

$$\frac{a_{W1} F_1}{1 + \sum_{j\neq 1}^n h_{1j}} = \cdots = \frac{a_{Wk} F_k}{1 + \sum_{j\neq k}^n h_{kj}} = \cdots = \frac{a_{Wn} F_n}{1 + \sum_{j\neq n}^n h_{nj}} \tag{21}$$

The numerator of each fraction in Eq. 21 deals with the homogeneous properties of the respective phase, while the denominator accounts for the hurdles (or free passages) related to the water exchanges with next neighboring phases. Limiting the discussion to a two-phase system, a steady state (no neat inter-phase water displacements) obeys the condition

$$\frac{a_{W1} F_1}{1 + (h_{12} + h_{21})} = \frac{a_{W2} F_2}{1 + (h_{12} + h_{21})} \tag{22}$$

If $F_1 = F_2$, then $a_{\mathrm{W1}} = a_{\mathrm{W2}}$: which corresponds to a true thermodynamic equilibrium. If $F_1 \neq F_2$, then the steady condition implies that $(a_{\mathrm{W1}}/a_{\mathrm{W2}}) = (F_2/F_1)$: the two phases can host solutions with different a_W, as the inter-phase hurdles reduce the rate of water exchanges, depending on the exponents α_1 and α_2 (see Eq. 19). If either h_{12} or $h_{21} = \infty$, Eq. 22 is meaningless as the two phases actually are isolated from each other.

5 Conclusions

Soft materials and very viscous systems are often far from the true thermodynamic equilibrium, because of residual strains and mesoscopic heterogeneous regions. Their metastable state can last for a long period and produce experimental evidences that depend on the "waiting time" between preparation and investigation, namely the age of the system.

Literature reports a number of theoretical and experimental approaches to relate relaxation processes at the molecular scale with the relaxation of long-range strains that keep the system far from the thermodynamic equilibrium. The most recent papers describe equilibrium and steady metastable states with sophisticated theoretical visions and mathematical treatments.

The present paper suggests a much simpler phenomenological approach for viscous homogeneous aqueous systems through a modified expression of the chemical potential of water. Taking advantage of the Gibbs and Adam relationships between viscosity and excess configurational entropy, the proposed approach suggests a modified expression of the chemical potential of water by addition of an extra term that accounts for the effects of the relative viscosity, like the extra drop of the freezing point of aqueous solution of polymers. The approach leads to formal expressions that reproduce the Eyring's equation for the viscosity of flowing liquids and Angell's Arrhenius like equation for the viscosity of "strong liquids".

Heterogeneous aqueous systems, like simple physical hydrogels, can find a reliable representation in a "dynamic" phase diagram. The gel/sol "transition would imply exchange of water between aqueous phase and amorphous hydrated components, at constant overall composition of the system. This allows an interpretation of the commonly observed hysteresis that characterizes this process.

As for more complex multiphasic systems, one has to take into account hurdles that can reduce the rate of water exchanges between next neighboring phases. These can delay the attainment of a steady (and possibly equilibrium) condition or actually isolate some aqueous phase from the surrounding medium: one can envisage the coexistence of aqueous phases with different a_W. In such cases, ad hoc experimental techniques allow the achievement of some information about the state of water in each single phase.

Appendix

Equivalence of WLF and VTF Equations [12–14]

Taking into account that either equation is empirical and aims at the description of the relaxation time at the temperature T, with reference to T_g and T_o, for WLF and VTF, respectively, one may put:

WLF

$$\tau_R(T) = \tau_R(T_g)\exp\left[-\frac{C_1(T-T_g)}{C_2+(T-T_g)}\right] \tag{A1}$$

VTF

$$\tau_R(T) = \tau_R(\infty)\exp\left(\frac{B}{(T-T_o)}\right) \tag{A2}$$

For $T=T_g$, Eq. 5 leads to

$$\tau_R(T_g) = \tau_R(\infty)\exp\left(\frac{B}{(T_g-T_o)}\right) \tag{A3}$$

that can be replaced in Eq. A1 which in combination with A2 gives

$$\tau_R(T) = \tau_R(\infty)\exp\left(\frac{B}{(T_g-T_o)}\right)\exp\left[-\frac{C_1(T-T_g)}{C_2+(T-T_g)}\right] = \tau_R(\infty)\exp\left(\frac{B}{(T-T_o)}\right) \tag{A4}$$

The eventual result is as follows:

$$\frac{C_2 + \left(T - T_g\right)}{C_1} = \frac{\left(T - T_o\right)\left(T_g - T_o\right)}{B} \tag{A5}$$

Putting $T = T_o$, one gets

$$C_2 = \left(T_g - T_o\right) \tag{A6}$$

and

$$B = C_1 C_2 \tag{A7}$$

Taking into account that $(T - T_o) = (T - T_g) + (T_g - T_o) = C_2 + (T - T_g)$, Eqs. A6 and A7 state the formal equivalence of the WLF and VTF equations. However, it is important to recall that the WLF equation seems more adequate for polymer solutions at $(T_g + 100\ \mathrm{K}) > T > T_g$ and therefore does not cover the (T_o, T_g) range, while the VTF equation holds for $T > T_o$ and describes the experimental evidence of many glass-forming systems [14].

Equation 6 reveals that C_1 corresponds to the abrupt change of the order of magnitude of τ_R on crossing the glass transition threshold T_g [15]:

$$\log_{10}\left[\frac{\tau_R\left(T_g\right)}{\tau_R(\infty)}\right] = \log_{10}\left[\frac{\eta\left(T_g\right)}{\eta(\infty)}\right] = \frac{C_1}{2.3} \tag{A8}$$

which, for 8 orders of magnitude viscosity drop, implies for C_1 a "universal" value around 17 (while $C_2 \approx 50$ °C) [15].

When combined with Eqs. 1, A6 and A7, A8 leads to

$$S_c = \frac{C}{B}\frac{T - T_o}{T} = \frac{C}{C_1 C_2}\left(1 - \frac{T_o}{T}\right) = \frac{C}{\left(T_g - T_o\right)\ln\left(\frac{\tau_{R,g}}{\tau_{R,\infty}}\right)} \tag{A9}$$

where T_o is the temperature at which $S_c = 0$, possibly coincident with the Kauzmann temperature, T_K, where the entropy of the undercooled liquid becomes equal to that of the thermodynamically stable solid phase.

Author Contributions Alberto Schiraldi wrote the manuscript and prepared all the figures.

Funding No funds were received for the activities related to this paper.

Declarations

Conflict of interest Alberto Schiraldi, declares that this paper does not imply any conflict of interest.

References

1. Guggenheim, E.A.: Themodynamics: An Advanced Treatment for Chemists and Physicists. North Holland Physics Publisher, Amsterdam (1986)
2. Jones, G., Dole, M.J.: The viscosity of aqueous solutions as a function of the concentration. Am. Chem. Soc. **51**, 2950–2964 (1929)

3. Schiraldi, A., Fessas, D.: Knudsen thermogravimetry approach to the thermodynamics of aqueous solutions. J. Chem. Thermodyn. **62**, 79–85 (2013)
4. Greenspan L.: Humidity fixed points of binary saturated aqueous solutions. J. Res. Nat. Bureau Stand. 81 (1977).
5. Kirinčić, S., Klofutar, C.: Viscosity of aqueous solutions of poly(ethylene glycol)s at 29815 K. Fluid Phase Equilib. **155**, 311–325 (1999).
6. Pleiner, H., Brand, H.R.: A two-fluid model for the formation of clusters close to a continuous or almost continuous transition. Rheol. Acta **60**, 675–690 (2021)
7. Gibbs, J.H., DiMarzio, E.A.: Nature of the glass transition and the glassy state. J. Chem. Phys. **28**, 373–383 (1958)
8. Adam, G., Gibbs, J.H.: On the temperature dependence of cooperative relaxation properties in glass-forming liquids. J. Chem. Phys. **43**, 139–146 (1965)
9. Freed, K.F.: Communication: towards first principles theory of relaxation in supercooled liquids formulated in terms of cooperative motion. J. Chem. Phys. **141**(141102), 1–4 (2014)
10. Maxwell, J.C.: Phil. Mag. **35**, 133 (1868)
11. Ito, K., Moynihan, C.T., Angell, C.A.: Thermodynamic determination of fragility in liquids and a fragile-to-strong liquid transition in water. Nature **398**, 492–495 (1999)
12. Williams, M.L., Landel, R.F., Ferry, J.D.: The temperature dependence of relaxation mechanisms in amorphous polymers and other glass-forming liquids. J. Am. Chem. Soc. **77**, 3701–3707 (1955)
13. Angell, C.A., Smith, D.L.: Test of the entropy basis of the Vogel-Tammann-Fulcher equation. Dielectric relaxation of polyalcohols near T_g. J. Phys. Chem. **86**, 3845–3852 (1982)
14. Ikeda, M., Aniya, M.: Understanding the Vogel–Fulcher–Tammann law in terms of the bond strength–coordination number fluctuation model. J. Non Cryst. Solids **371–72**, 53–57 (2013)
15. Schiraldi, A.: Comparison between WLF and VTF expressions and related physical meaning. In: Levine, H. (ed.) Amorphous Food and Pharmaceutical Systems, pp. 131–136. The Royal Society Chemistry (2002).
16. Angell, C.A.: Liquid fragility and the glass transition in water and aqueous solutions. Chem. Rev. **102**, 2627–2650 (2002)
17. Martinez, L.-M., Angell, C.A.: A thermodynamic connection to the fragility of glass-forming liquids. Nature **410**, 663–667 (2001)
18. Klein, I.S., Angell, C.A.: Excess thermodynamic properties of glass forming liquids: the rational scaling of heat capacities, and the thermodynamic fragility dilemma resolved. J. Non-Cryst. Solids **451**, 116–123 (2016)
19. Eyring, H.J.: Viscosity, plasticity, and diffusion as examples of absolute reaction rates. J. Chem. Phys. **4**, 283–291 (1936)
20. Kincaid, J.F., Eyring, H.J., Stearn, A.E.: The theory of absolute reaction rates and its application to viscosity and diffusion in the liquid state. Chem. Reviews **28**, 301–365 (1941)
21. Schottky, W.: Chemie der elementar prozesse aufbau der materie. Zeits.-P. Chem. **B29**, 335–355 (1935)
22. Frenkel, Y.: Über die Wärmebewegung in festen und flüssigen Körpern. Z. Phys. **35**, 652–669 (1926)
23. Chen, C., Zeng, H., Deng, Y., Yan, J., Jiang, Y., Chen, G., Zu, Q., Sun, L.: A novel viscosity-temperature model of glass-forming liquids by modifying the eyring viscosity equation. Appl. Sci. **10**(428), 1–9 (2020). https://doi.org/10.3390/app10020428
24. Schrodt, J.T., Akel, R.M.: Binary liquid viscosities and their estimation from classical solution thermodynamics. J. Chem. Eng. Data **34**, 8–13 (1989)
25. Tong, H., Tanaka, H.: Revealing hidden structural order controlling both fast and slow glassy dynamics in supercooled liquids. Phys. Rev. X **8**(011041), 1–18 (2018). https://doi.org/10.1103/PhysRevX.8.011041
26. Mishin, Y.: Thermodynamic theory of equilibrium fluctuations. Ann. Physics **363**, 48–97 (2015)
27. Karmakara, S., Dasgupta, C., Sastry, S.: Growing length and time scales in glass-forming liquids. PNAS **106**, 3675–3679 (2009)
28. Ghoshal, D., Joy, A.: Shear stresses of colloidal dispersions at the glass transition in equilibrium and in flow. Phys. Rev. **102**, 062605 (2020)
29. Johari, G.P.: Specific heat relaxation-based critique of isothermal glass transition, zero residual entropy and time-average formalism for ergodicity loss. Thermochim. Acta **523**, 97–104 (2011)
30. Barrat, J.-L., Feigelman, M., Kurchan, J., Dalibard, J. (eds.): Slow Relaxations and Non-equilibrium Dynamics in Condensed Matter. Euro Summer School, Session LXXVII, 1–26 July 2002, NATO Advanced Study Institute. EDP Sci. Springer Publication (2003)
31. Thirumalai, D., Mountain, R.D.: Activated dynamics, loss of ergodicity, and transport in supercooled liquids. Phys. Rev. E **47**, 479–489 (1993)

32. Cipelletti, L., Ramos, L.: Slow dynamics in glassy soft matter. J. Phys. **17**, 253–285 (2005)
33. Slade, L., Levine, H.: Beyond water activity: recent advances based on an alternative approach to the assessment of food quality and safety. Crit. Rev. Food Sci. Nutr. **30**, 115–360 (1991)
34. Corti, H.R., Angell, C.A., Auffret, T., Levine, H., Buera, M.P., Reids, D.S., Roos, Y.H., Slade, L.: Empirical and theoretical models of equilibrium and non-equilibrium transition temperatures of supplemented phase diagrams in aqueous systems (IUPAC Technical Report). Pure Appl. Chem. **82**, 1065–1097 (2010)
35. Crassous, J.J., Siebenbürger, M., Ballauff, M., Drechsler, M., Hajnal, D., Henrich, O., Fuchs, M.: Shear stresses of colloidal dispersions at the glass transition in equilibrium and in flow. J. Chem. Phys. **128**, 204902 (2008)
36. Fessas, D., Schiraldi, A.: State diagrams of arabinoxylan-water binaries. Thermochim. Acta **370**, 83–89 (2001)
37. Belton, P.S.: On the elasticity of wheat gluten. J. Cereal Sci. **29**, 103–107 (1999)
38. Schiraldi, A., Fessas, D.: Water properties in wheat ¯our dough I: classical thermogravimetry approach. Food Chem. **72**, 237–244 (2001)
39. Piazza, L., Schiraldi, A.: Correlation between fracture of semi-sweet hard biscuits and dough viscoelastic properties. J. Texture Studies **28**, 523–541 (1997)
40. Corredig, M., Alexander, M.: Food emulsions studied by DWS: recent advances. Trends Food Sci. Technol. **19**, 67–75 (2008)
41. Butler, M.F., Heppenstall-Butler, M.: Phase separation in gelatin/dextran and gelatin/maltodextrin mixtures. Food Hydrocolloids **17**, 815–830 (2003)
42. Paradossi, G., Chiessi, E., Barbiroli, A., Fessas, D.: Xanthan and glucomannan mixtures: synergistic interactions and gelation. Biomacromol. **3**, 498–504 (2002)
43. Schiraldi A. Unpublished data, available from the author.
44. San Biagio, P.L., Bulone, D., Emanuele, A., Palma-Vittorelli, M.B., Palma, M.U.: Spontaneous symmetry-breaking pathways: time-resolved study of agarose gelation. Food Hydrocolloids **10**, 91–97 (1996)
45. Boral, S., Bohidar, H.B.: Effect of water structure on gelation of agar in glycerol solutions and phase diagram of agar organogels. J. Phys. Chem B **116**, 7113–7121 (2012).
46. Voorhaar, L., Hoogenboom, R.: Supramolecular polymer networks: hydrogels and bulk materials. Chem. Soc. Rev. **45**, 4013–4031 (2016). https://doi.org/10.1039/c6cs00130k
47. Appel, E.A., del Barrio, J., Loh, X.J., Scherman, O.A.: Supramolecular polymeric hydrogels. Chem. Soc. Rev. **41**, 6195–6214 (2012)
48. van der Sman, R.G.M., Meinders, M.B.J.: Prediction of the state diagram of starch water mixtures using the Flory–Huggins free volume theory. Soft Matter. (2011). https://doi.org/10.1039/c0sm00280a.
49. Dawson, K.A., Foffi, G., Sciortino, F., Tartaglia, P., Zaccarelli, E.: Mode-coupling theory of colloids with short-range attractions. J. Phys. **13**, 9113–9126 (2001)
50. Hunter, G.L., Weeks, E.R.: The physics of the colloidal glass transition. Rep. Prog. Phys. **75**, 066501 (2012)
51. Sessoms, D.A., Bischofberger, I., Cipelletti, L., Trappe, V.: Multiple dynamic regimes in concentrated microgel systems. Phil. Trans. R. Soc. A **367**, 5013–5032 (2009)
52. Dauchot, O.: Ageing and the glass transition. Lect. Notes Phys. **716**, 161–206 (2007). https://doi.org/10.1007/3-540-69684-9_4
53. Ergun, R., Lietha, R., Hartel, R.W.: Moisture and shelf life in sugar confections. Crit. Rev-Food Sci. Nutr. **50**, 162–192 (2010)
54. Ellis, R.J.: Macromolecular crowding: obvious but underappreciated. Trends in Biochem. Sci. **26**, 597–604 (2001)
55. Tolostoguzov, V.B.: Thermodynamic Incompatibility of food macromolecules. In: Dickinson, E., Walstra, P. (eds.) Food colloids and polymers: stability and mechanical properties. R. Soc. Chem., Special Publication, N **113**, 94–102 (1993).
56. Hills, B.P.: Magnetic Resonance Imaging in Food Science. Wiley, New York (1998)
57. Hall, L.D., Amin, M.H.G., Evans, S., Nott, K.P., Sun, L.: Quantitation of diffusion and mass transfer of water by MRI. In: Berk, Z., Leslie, R.B., Lillford, P.J., Mizrahi, S., (eds.) Water Science for Food, Health, Agriculture and Environment, pp. 1255–1271. Technomic Publications Co, Lancaster (2001).
58. Ruan, R.R., Chen, P.L.: Water in Foods and Biological Materials. A Nuclear magnetic Resonance Approach. Technomic Publ Co, Lancaster (1998)
59. Rolandelli, G., Farroni, A.E., Buera, M.P.: Analysis of molecular mobility in corn and quinoa flours through 1H NMR and its relationship with water distribution, glass transition and enthalpy relaxation. Food Chem. **373**(1–9), 131422 (2022)

60. Mallamace, F., Corsaro, C., Mallamace, D., Vasi, S., Vasi, C., Stanley, H.E.: Thermodynamic properties of bulk and confined water. J. Chem. Phys. **141**, 141–150 (2014)
61. Hu, Y., Li, C., Tan, Y., McClements, D.J., Wang, L.: Insight of rheology, water distribution and in vitro digestive behavior of starch based-emulsion gel: impact of potato starch concentration. Food Hydrocolloids **132**, 107859 (2022)
62. Stecchini, M.L., Del Torre, M., Donda, S., Maltini, E., Pacor, S.: Influence of agar content on the growth parameters of *Bacillus cereus*. Int. J. Food Microb. **64**, 81–88 (2001)
63. Hills, B.P., Manning, C.E., Ridge, Y., Brocklehurst, T.: NMR water relaxation, water activity and bacterial survival in porous media. J. Sci. Food Agric. **71**, 185–194 (1996)